Available online at www.sciencedirect.com
SCIENCE DIRECT
Polymer 47 (2006) 357–366
polymer
www.elsevier.com/locate/polymer

Structure–property relationships in novel poly(imide-amide)–poly (ethylene glycol) hybrid networks

S. Kripotou [a], P. Pissis [a,*], P. Sysel [b], V. Sindelar [b], V.A. Bershtein [c]

[a] Department of Physics, National Technical University, Zografou Campus, 157 80 Athens, Greece
[b] Department of Polymers, Institute of Chemical Technology, Technicka 5, 16628 Prague 6, Czech Republic
[c] Ioffe Physico-Technical Institute of the Russian Academy of Sciences, 26 Polytechnicheskaya Str., 194021 St Petersburg, Russian Federation

Received 7 September 2005; received in revised form 26 October 2005; accepted 3 November 2005
Available online 28 November 2005

Abstract

Broadband dielectric relaxation spectroscopy (DRS), thermally stimulated depolarisation currents (TSDC), differential scanning calorimetry (DSC) and to a lesser extent water uptake measurements, were employed to investigate molecular mobility, morphology and crystallization/melting events of PEG in poly(imide-amide)–polyethylene glycol hybrid networks (PIA–PEG) with short ($M_n = 1000$ g/mol) and long ($M_n = 3400$ g/mol) PEG crosslinks. The results obtained suggest long range connectivity of the PEG component in the hybrids with short PEG crosslinks at PEG content higher than 40 wt% and in these with long PEG crosslinks at PEG content higher than 20 wt%. Crystallization of the PEG component is observed by DSC in the hybrids with the longer crosslinks at sufficiently high content of PEG, only. The glass transition temperature, T_g, of PEG component in the hybrids with the shorter PEG crosslinks is shifted to higher temperatures compared to that of the hybrids with longer PEG crosslinks, while suppression of the glass transition of the PEG component is observed in the hybrids with the shorter PEG crosslinks at PEG content lower than 40 wt%. The results are discussed in terms of constraints to segmental motion of the PEG crosslinks, imposed by fixed PEG chain ends on the rigid PI chains.

Keywords: Hybrid polymer networks; Molecular mobility; Dielectric techniques

1. Introduction

Polyimides (PIs) are high-performance polymers with excellent thermal stability, chemical resistance and mechanical, dielectric and adhesive properties, which find numerous applications in aerospace, microelectronics and membrane technologies [1,2]. The use of PIs in membrane technologies for the separation of heat solvent-containing air streams is based on good selectivity combined with good thermal, mechanical and solvent resistance [1,3]. However, low permeability of PIs for gases and organic vapors is a serious disadvantage for such applications [1,4,5].

The permeability of PIs for small molecules can be improved by incorporation of flexible polymer chains into their structure. In fact, membranes based on poly(ether-imide) were successfully employed for the separation of organic vapors from air gases [6,7].

In a series of papers, we investigated over the last 5 years the performance of PIs modified by the incorporation of flexible polymer chains. This work has been recently reviewed [8]. Linear random or block poly(imide-dimethylsiloxane) (PI-PDMS) copolymers showed improved membrane properties, compared to pure PI, combined, however, with irreversible changes of the copolymers structure induced by the penetration of the organic vapors [9,10]. However, the overall stability can be improved by crosslinking the linear chains into a three-dimensional network [11]. In fact, PI-PDMS hybrid networks could be prepared, where short PDMS chains with both ends chemically bound to the PI phase formed spherical domains of nanometer size [12,13]. In a next step, poly(imide-amide)–poly(ethylene adipate) (PIA–PEA) hybrid networks were prepared and systematically investigated in terms of structure–property relationships [14,15] and membrane properties [3]. The results showed pronounced heterogeneity of segmental dynamics and improved membrane performance of the hybrid networks.

Thus, our previous work indicated that modification of PI by flexible crosslinks is a promising route for developing high-performance membranes having both increased resistance and sufficient permeability and selectivity for gases and organic

* Corresponding author. Tel.: +30 210 772 2986; fax: +30 210 772 2932.
E-mail address: ppissis@central.ntua.gr (P. Pissis).

0032-3861/$ - see front matter © 2005 Elsevier Ltd. All rights reserved.
doi:10.1016/j.polymer.2005.11.012

vapors. The character of polymer chains influences both diffusivity (by their flexibility) and sorption (by their chemical composition). From this point of view it has been useful to substitute PEA used in our previous work [14,15] by poly(ethylene glycol) as crosslinker.

In the work presented here we follow the same concept of modification of PI by flexible crosslinks and report on the preparation of poly(imide-amide)–poly(ethylene glycol) (PIA–PEG) hybrid networks and the investigation of structure–property relationships in these materials. Special attention is paid to the investigation of molecular dynamics as a function of composition and PEG molar mass, the reason for that being that molecular mobility determines to a large extent the transport processes through membranes. Differential scanning calorimetry (DSC), dielectric relaxation spectroscopy (DRS), thermally stimulated depolarization currents (TSDC) techniques and water uptake measurements are employed to that aim and the results are discussed in terms of morphology, molecular mobility and crystallization of PEG in the hybrid networks.

Besides their technological significance, the materials under investigation are interesting also from the fundamental point of view, in particular with respect to the study of the chain dynamics of the short, flexible PEG crosslinks. Thus, special attention is paid to the investigation, by DSC, DRS and TSDC, of the dynamics of the PEG crosslinks in the hybrids. The results can be discussed in terms of nanoscale confinement and of constraints imposed by fixing the PEG chain ends [8,13] and contribute to a better understanding of chain dynamics in nanostructured polymeric systems [16].

2. Experimental

2.1. Materials

The materials were prepared from poly(amic acid) (PAA) based on pyromellitic dianhydride (PMDA) and 4, 4′-oxydianiline (ODA), as the PI precursor, and 4-methyl-1, 3 phenylene diisocyanate terminated poly(ethylene glycol) (TDI–PEG). PEG with two different number average molar masses, $M_n = 1000$ and 3400 g/mol, were used.

PAA (PMDA–ODA) with uncontrolled molecular weight was prepared by the reaction of equimolar amounts of a dianhydride and a diamine in the solvent, 1-methyl-2-pyrrolidone (NMP, Merck) (solid content 10 wt%) at room temperature for 24 h. The PEG terminated with TDI (TDI–PEG) were prepared by the reaction of TDI and PEG in a molar ratio 3:1. The 10 wt% solution of PEG in toluene was allowed to react at room temperature for 2 h. Finally, the phenol was added into the mixture (molar ration TDI–PEG: PhOH = 1:2) and it was allowed to react for additional 3 h. The solution was precipitated into diethylether and the collected product was dried at room temperature to constant weight under reduced pressure. Pyromellitic dianydride (PMDA) was heated overnight at 160 °C in vacuum before use. 4,4′-Oxydianiline (ODA), and phenol (all Aldrich) were used as received. NMP was distilled in vacuum over phosphorus pentoxide and stored in an inert atmosphere.

PAA solution in NMP and TDI–PEG were mixed at room temperature for 2 h in various weight ratios. The PAA/TDI–PEG mixtures (or pure components) in NMP were cast onto a glass or teflon plate. After evaporating the solvent, the films based on the mixtures were subjected to thermal treatment at 150, 200 and 250 °C for 1, 2 and 1 h, respectively. The final films were slightly opalescent with a thickness of ca. 50–100 μm.

During the thermal treatment, phenol was released and the deprotected isocyanate groups of TDI–PEG reacted with the carboxylic groups of PAA (PMDA–ODA) with formation of amide groups. Consequently, two reactions, both PAA imidization and crosslinking (hybridization of both components), proceeded in parallel on heating (Scheme 1).

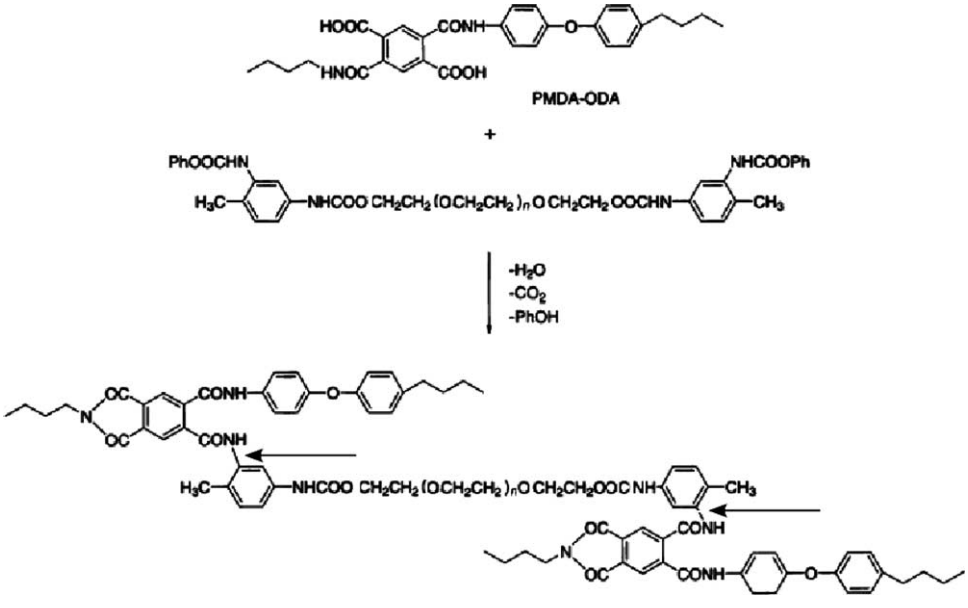

Scheme 1.

As a result, the networks formed were quite complicated in their structures, and contained basically imide groups in backbone and ester groups in crosslinks and also the amide and urethane groups in backbone and crosslinks, respectively.

Besides pure linear PI two series of hybrid networks were prepared, with short (M_n = 1000 g/mol) and long (M_n = 3400 g/mol) PEG crosslinks and PIA/PEG weight ratios of 80/20, 60/40, 50/50, 40/60 and 20/80 for both series. In the rest of text the samples with MW of PEG 1000 and 3400 g/mol will be designated as K and D, respectively, while the number accompanying the letters K and D refers to wt% content of PEG.

2.2. Experimental methods

For DRS measurements the complex dielectric permittivity, $\varepsilon^* = \varepsilon' - i\varepsilon''$, was determined as a function of frequency (10^{-1}–10^6 Hz) in the temperature range from 130 to 350 K (controlled to better than $\pm$0.1 K). A Schlumberger frequency response analyzer (FRA, SI 1260) supplemented by a buffer amplifier of variable gain (Chelsea dielectric interface) in combination with the Novocontrol Quatro Cryosystem were used. The samples were circular films of 20 mm diameter and thickness between 50 and 100 μm.

The TSDC measurements were performed on circular films with 14 mm in diameter. The sample was inserted between the brass plates of a capacitor and polarized by the application of electric field E_p at temperature T_p for time t_p, which was large in comparison with the relaxation time at T_p of the dielectric dispersion under investigation. With the electric field still applied, the sample was cooled to temperature T_0 (which was sufficiently low to prevent depolarization by thermal excitation), and then was short-circuited and reheated at a constant rate b. A discharge current was generated as a function of temperature, which was measured with a sensitive electrometer [18]. The equivalent frequency f of TSDC measurements [13] spans $10^{-4} < f < 10^{-2}$ Hz, i.e. it is similar to those of DSC measurements. High TSDC sensitivity allows the detection of weak relaxations.

A homemade experimental apparatus for TSDC measurements was used, which operated over the temperature range from 77 to 300 K [13]. Typical conditions were E_p = 6 kV/cm for the polarizing field, T_p = 300 K for the polarization temperature, t_p = 5 min for the polarization time, 6 K/min for the cooling rate to T_0 = 88 K, and b = 3 K/min for the heating rate.

Differential scanning calorimetry (DSC) was employed to investigate the glass transition and the melting behavior of the PEG component in the networks. The measurements were performed over the temperature range 120–500 K using the Perkin–Elmer DSC-2 apparatus in nitrogen atmosphere at a heating rate of 20 K/min. The first DSC scan indicated some endothermic contribution in the temperature range 300–400 K associated with removing of water. Therefore, measurements were performed in a second heating scan after heating the sample up to 500 K followed by rapid cooling down to 120 K at a rate of 320 K/min.

Equilibrium water uptakes were measured at room temperature. The samples were allowed to equilibrate to constant weight in a desiccator with constant relative humidity RH = 0.97 (saturated K_2SO_4 aqueous solution). A value of RH lower than 1 was chosen in order to avoid condensation of water on the samples. The water content, h, defined as the ratio of the weight of water to the weight of the dry sample, was determined by weighing. Dry weights were determined after drying the samples in vacuum for 24 h at120 °C.

3. Results and discussion

3.1. Morphology

Fig. 1 shows results of DRS measurements in the two series of hybrid networks at 298 K: the real part ε' of the complex dielectric permittivity $\varepsilon^*(f) = \varepsilon'(f) - i\varepsilon''(f)$ and Ac conductivity σ_{Ac} (actually real part σ'_{Ac} of the complex Ac conductivity) against frequency f. $\sigma_{Ac}(f)$ has been calculated by [19]

$$\sigma_{Ac}(f) = \varepsilon''(f)\varepsilon_0 2\pi f \quad (1)$$

where $\varepsilon''(f)$ the measured dielectric loss and ε_0 the permittivity of free space. In each series we observe a general tendency of increasing values of ε' and σ_{Ac} with increasing fraction of PEG in the networks. The high values of $\varepsilon'(f)$ at low frequencies in the PEG-rich networks do not reflect bulk properties. They arise from space charge and/or electrode polarization related with high values of electrical conductivity [20]. Conductivity effects become less important at higher frequencies and a tendency for ε' of the hybrid networks to level off at frequencies higher than 100 kHz is observed in Fig. 1. It is interesting to note in this connection a recent report on the preparation of nanoporous polyimide with grafted PEG side chains and its investigation as potential low-permittivity material [21]. In the PEG-rich samples $\sigma_{Ac}(f)$ becomes independent of frequency at low frequencies (conductivity plateau, Dc conductivity σ_{Dc}), whereas it deviates to higher values at higher frequencies, as commonly observed in many ionic conductors [22]. Finally, for the same fraction of PEG, conductivity effects, both in $\varepsilon'(f)$ and in $\sigma_{Ac}(f)$, are stronger in the hybrids with the longer crosslinks, compare, for example, in Fig. 1 samples K50 and D50 with each other.

The broad frequency range of DRS measurements allows, in many cases, to conclude on the morphology of the samples under investigation. On the basis of the results shown in Fig. 1 the samples can be classified into two groups: PIA-rich samples (pure PI, K20, K40, D20) and PEG-rich samples (K50, K60, K80, D40, D50, D80, pure PEG). No conductivity effects are observed in $\varepsilon'(f)$ and no tendency for a σ_{Dc} plateau at low frequencies in the σ_{Ac} (f) plot for the samples of the first group. For the samples of the second group, on the contrary, conductivity effects in $\varepsilon'(f)$ are rather strong, increasing with increasing PEG content and PEG chain length, and a plateau appears in the $\sigma_{Ac}(f)$ plot, indicating Dc conductivity, which also increases as PEG content increases. Thus, the results in Fig. 1 suggest that PEG forms a continuous phase in

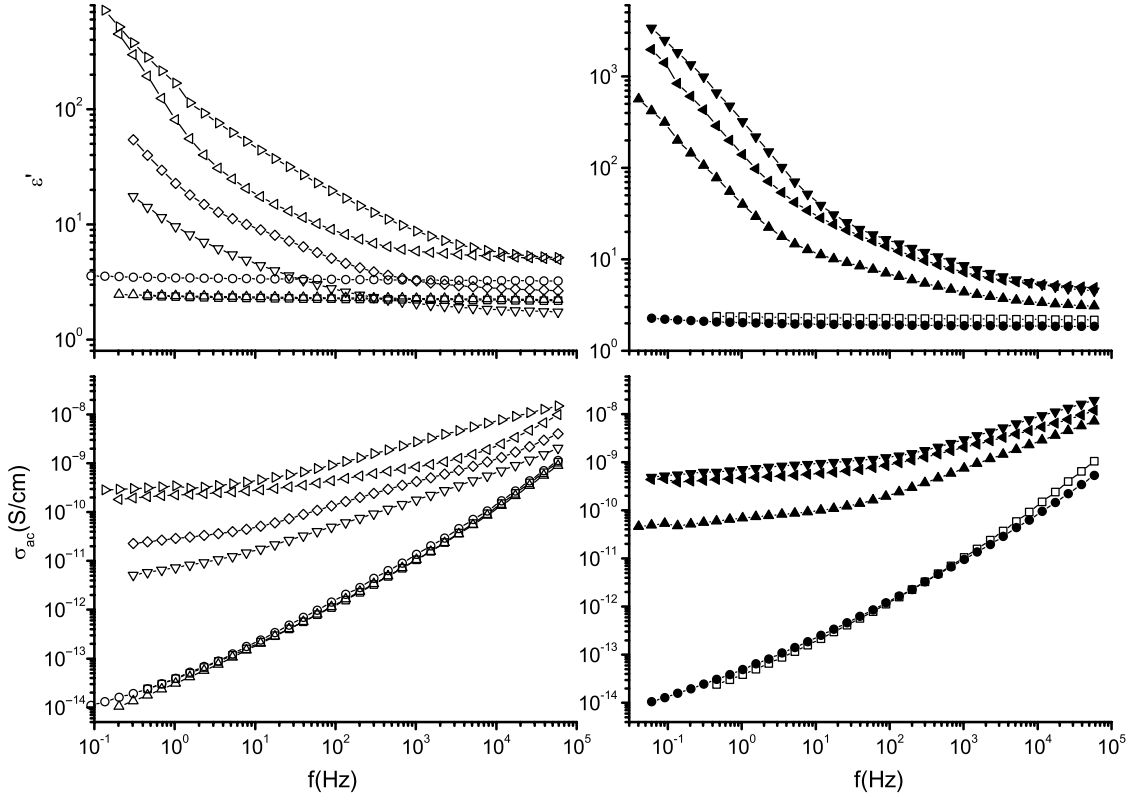

Fig. 1. Real part of dielectric permittivity ε' and of Ac conductivity σ_{Ac} against frequency f of pure PI (□), K20 (○), K40 (△), K50 (▽), K60 (■), K80 (◁), pure PEG_{1000} (▷), D20 (●), D40 (▲), D50 (▼), and D80 (◀) at 298 K.

the PEG-rich samples of group 2 and a discrete one (spatially isolated domains) in the PI-rich samples of group 1.

Conductivity effects can be further followed by using the modulus formalism. The complex electric modulus M^* is defined by [23]

$$M^*(f) = \frac{1}{\varepsilon^*(f)} \tag{2}$$

Electrode and space charge polarization are effectively suppressed in the modulus formalism. A plot of $M''(f)$ shows a peak in the frequency region where $\sigma_{Ac}(f)$ deviates from the frequency-independent plateau value of σ_{Dc} (conductivity relaxation [24]), as represented for selected samples of the K and D series and pure PEG of molecular weight 1000 g/mol in Fig. 2. The frequency f_{max} of this peak defines the conductivity relaxation time τ_{cond} by

$$2\pi f_{max}\tau_{cond} = 1 \tag{3}$$

The inset to Fig. 2 shows the Arrhenius plot of that frequency for the samples indicated on the plot. We observe again the classification of samples into two groups, as described above on the basis of Fig. 1, in particular the similarity in the behavior of samples K20 and K40. Please note, however, the extension now of that classification to variable temperature, as compared to Fig. 1.

Sorption and diffusion of water molecules (of small molecules, in general) may reflect properties of morphology in multicomponent polymeric systems on the basis of differentiation in the interaction of the absorbed molecules with the two components. Table 1 shows results for the water content h of selected samples of the two series at room temperature and relative humidity 0.97. Water uptake increases in general in the hybrid networks, as compared to pure PI, since PEG is more hydrophilic than PI. However, we observe in Table 1 the distinctly different behavior of samples K40 and D40, which have the same composition but different PEG chain length: water uptake in sample K40 is similar to that of pure PI, whereas it is significantly higher in sample D40. This result

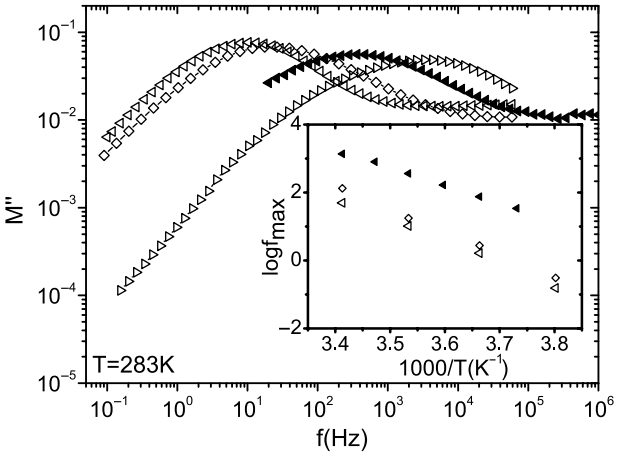

Fig. 2. Imaginary part of dielectric modulus M'' against frequency f for pure PEG_{1000} (▷), K80 (◁), K60 (◇), and D80 (◀) at 283 K. The inset shows the corresponding Arrhenius plot of the conductivity relaxation.

Table 1
Water content h at 298 K and relative humidity 0.97 of selected samples

Samples	*h*
PI	0.0490
K40	0.0490
D40	0.132
D50	0.198
K60	0.131
K80	0.297
D80	0.123

indicates that PEG forms a continuous phase in D40, which can swell on the absorption of water. The result for K40, on the contrary, is consistent with either formation of a separate, discrete PEG phase confined in the rigid PIA matrix [25], or mixing of two components. DSC results to be reported below may help to further clarify this point. An unexpected result in Table 1 is the drop of *h* for sample D80 below that for D50 and close to that for D40. Results, to be reported later, show that PEG partly crystallizes in the samples of the *D* series with more than 40 wt% PEG and that the degree of crystallinity increases with increasing PEG fraction. Bearing in mind that the ability to absorb water decreases significantly on crystallization, the reduction of *h* in D80 can be explained by the fact that a significant part of PEG crystallizes in this sample.

3.2. Molecular mobility

Fig. 3 shows DSC thermograms (second scans) in the glass transition region of the PEG component. For clarity, thermograms for different samples have been shifted on the vertical axis. The glass transition of the PEG component is manifested as a step in the thermograms. The glass transition of the PI component is at much higher temperatures, 550–600 K [8], and will not be further studied here. For each thermogram in Fig. 3 the glass transition temperature T_g at the half-height of the heat capacity step and the onset and completion temperatures of the transition ranges [26] have been determined and are also indicated on the plots. We observe in Fig. 3 that T_g of PEG is in the range 223–228 K in the hybrids with the longer crosslinks (series D), whereas it is shifted to higher temperatures, 236–252 K, in the PEG-rich hybrids with the shorter crosslinks (series K). No systematic variation of T_g with the PEG content is observed in neither of the two series. The most striking result in Fig. 3, next to the shift of T_g to higher temperatures in the K series, is the absence of any heat capacity jump in the samples K20 and K40. Homogeneous mixing of the two components, giving rise to a single glass transition between those of the two single components, or total suppression of the glass transition of the PEG component due to constraints imposed by the rigid PI component [8] may be the reason for that absence. DSC measurements in the region of the glass transition of the PI component give for these two samples T_g values of 565 and 555 K, respectively. These high values are not consistent with mixing of the two components, indicating that the glass transition of PEG is suppressed in these samples, whereas it is observed in the corresponding samples of the D series. DSC measurements in the temperature region of crystallization/melting of PEG, to be reported in details elsewhere, confirmed also by DRS measurements to be reported below, show that crystallization/melting events of PEG are observed only in the hybrids with the longer crosslinks.

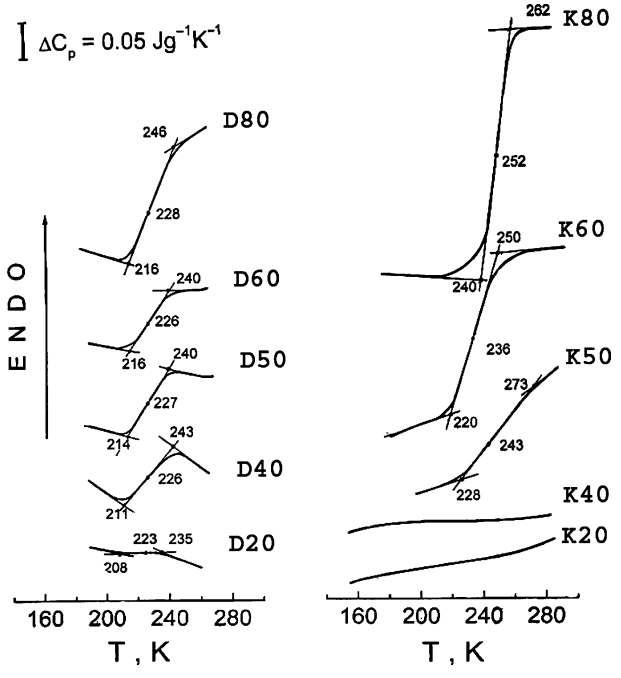

Fig. 3. DSC curves obtained in the region of PEG glass transition (second scans) for the samples indicated on the plot at a heating rate of 20 K/min.

The DSC results presented in Fig. 3 correlate well with the DRS results at room temperature shown in Fig. 1. The suppression of the glass transition of the PEG component in the samples K20 and K40 (Fig. 3) is in agreement with the fact that no conductivity effects were observed for these samples in the $\varepsilon'(f)$ and $\sigma_{Ac}(f)$ plots of Fig. 1, both results indicating reduced mobility of the PEG chains. Also, the very small heat capacity jump at the glass transition of the PEG component for the sample D20, as compared to sample D40, is consistent with the absence of conductivity effects for this sample in Fig. 1. We will take on this point again later in the next section on the basis of results for the crystallization of the PEG component in the hybrids.

It is interesting to compare the DSC results presented above with DSC results obtained with PIA–PEA hybrid networks [14]. In the PIA–PEA hybrids with molar mass of PEA 1300 and 2700 g/mol crystallization/melting events of PEA were observed only for the longer crosslinks, similar to the PIA–PEG hybrids under investigation here. Also, glass transition and crystallization/melting of PEA in the hybrids with longer crosslinks were suppressed at low PEA content. In the PIA–PEA hybrids with the shorter crosslinks multiple T_gs were observed, which were shifted to higher temperatures with respect to the hybrids with the longer crosslinks. Thus, the results obtained here with the PIA–PEG hybrids resemble strongly those obtained with the PIA–PEA in our previous work [14]. These results can be explained in terms of

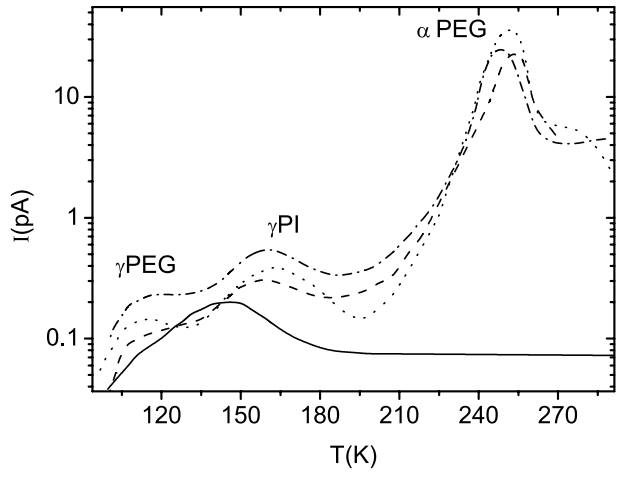

Fig. 4. TSDC thermograms obtained with pure PI (solid line), K50 (dashed line), K60 (dotted line) and K80 (dashed dotted line).

the constraining influence of the rigid PIA component on the dynamics of the softer PEG component due to covalent anchoring of the TDI–PEG component at both ends to the former, as indicated by arrows in Scheme 1. We will come back to this point later in this section by discussing the results of dielectric measurements.

Fig. 4 shows TSDC thermograms obtained with samples of the K series in the temperature range 100–275 K and, for comparison, a thermogram obtained with pure PI in the same temperature range. The thermograms are representative also for the other samples of the K series and for those of the D series. Compared with the more familiar DRS plots of Fig. 1, the TSDC thermograms correspond to plotting dielectric loss ε'' against temperature T at a constant frequency f in the range 10^{-2}–10^{-4} Hz. Three peaks are observed in Fig. 4, corresponding, in the order of increasing temperature, to the γ relaxation of PEG, the γ relaxation of PI, and the α relaxation, associated with the glass transition, of PEG.

The γ TSDC peak of PEG is located at around 115 K. In agreement with this interpretation, the peak is not present in the thermogram of pure PI, whereas its magnitude, which is a measure of the strength of the corresponding relaxation, i.e. of the number of molecular units participating to the relaxation [18], increases with increasing amount of PEG in the hybrids. For low PEG contents, the peak is expressed as a shoulder on the low-temperature side of the stronger (please note the logarithmic scale on the vertical axis) γ peak of PI. The temperature position of the peak, which gives the time scale of the corresponding relaxation [18], does not practically change with composition. In agreement with previous dielectric results obtained with polyethers and polyesters [15,27], the γ relaxation of PEG is attributed to crankshaft motions of methylene sequences $(CH_2)_n$. The γ peak of PI is located at about 145 K in the TSDC thermogram of pure PI in Fig. 4, in agreement with previous TSDC results obtained with PI-containing systems [13,15]. The γ relaxation of PI is attributed to non-cooperative torsional vibrations of the imide cycles [15,27]. The peak is shifted to higher temperatures in the hybrids, by about 10–15 K, indicating that the γ relaxation of PI is slightly slowed down in the hybrids. A pronounced effect of hybridization on the magnitude of the relaxation is observed in Fig. 4. Surprisingly, at a first glance, the height of the peak increases in the hybrids with increasing PEG content, i.e. with decreasing amount of PI, by a factor up to five in Fig. 4. These results are, however, in agreement with dielectric (TSDC and DRS) results obtained with other hybrid systems containing PI: PI–PDMS hybrid networks, where the γ relaxation was found, by both TSDC and DRS, to increase in magnitude and to become slightly slower in the hybrids, as compared to pure PI [13]; hybrid PI-silica nanocomposites, where the γ relaxation was found, by both TSDC and DRS, to increase significantly in magnitude without any significant change of the time scale, as compared to pure PI [28]. Similar to the results in the other hybrid systems [13,28], the TSDC results for the γ relaxation of PI in the PIA–PEG hybrids can be explained by loosened molecular packing of the PI chains, arising from the constraints imposed by the covalent bonds to PEG, and resulting in increase of free volume.

The TSDC α peak, associated with the glass transition of PEG (obviously not observed in the thermogram of pure PI) is located at about 250 K in the samples of the K series with more than 40 wt% PEG in Fig. 4 and at lower temperatures, in the range 230–245 K, in the samples with the longer crosslinks (series D). No α peak is observed in the thermograms of the samples K20 and K40, in agreement with the DSC results, the peaks at higher temperatures, in the range of 260–280 K, by more than one order of magnitude smaller than the TSDC α peaks, being associated with conductivity effects [13,15]. Thus, the temperature position of the TSDC α peak is similar to T_g measured by DSC in Fig. 1, reflecting the fact that the time scale of the two techniques is similar (10^{-2}–10^{-4} Hz) [18,26], and providing evidence for similar spatial scale of the molecular motions giving rise to the response in both techniques [29]. The temperature position and the magnitude of the TSDC α peak do not vary systematically with composition in neither of the two series of the hybrids. The first observation is in agreement with the DSC results in Fig. 3. The second observation and the rather high values of the magnitude of the peak suggest that conductivity effects contribute to the peak, as often observed in TSDC measurements in polymeric systems with rather high values of ionic conductivity [18].

Molecular mobility was further followed by DRS. Measurements were performed isothermally at several temperatures to systematically follow the three relaxations observed also by TSDC, i.e. the secondary γ relaxations of PI and of PEG and the α relaxation of PEG. Before presenting the analysis of these measurements, we show in Fig. 5 an isochronal (constant frequency) plot of dielectric loss ε'' against temperature for sample K80 at 100 Hz. This plot has been constructed from the isothermal $\varepsilon''(f)$ measurements. It is representative for the hybrid networks and makes possible a direct comparison of DRS and TSDC results, providing further evidence for the TSDC results presented above. Three loss peaks are observed in Fig. 5, in the order of increasing temperature, the γ relaxation of PEG, the γ relaxation of PI, and the α relaxation

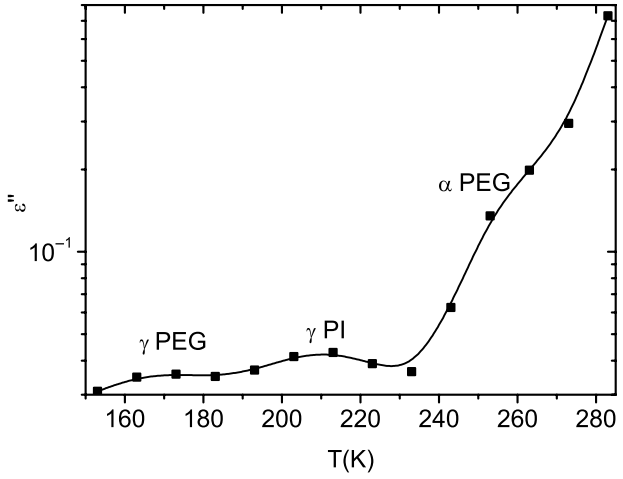

Fig. 5. Isochronal (constant frequency, $f=100$ Hz) plot of dielectric loss ε''; against temperature T for sample K80.

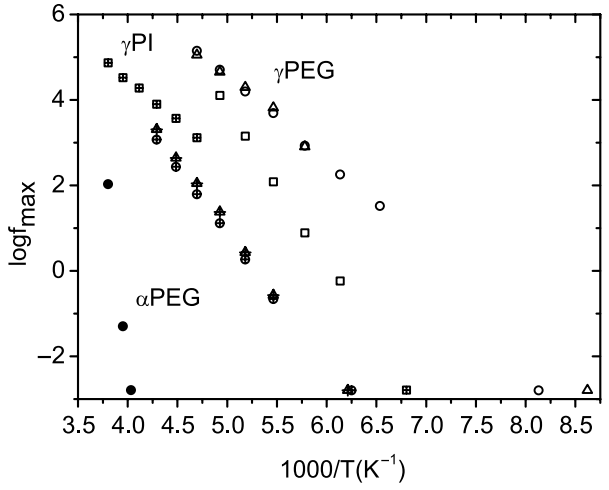

Fig. 6. Arrhenius diagram of the γ relaxation of PEG and the γ relaxation of PI for pure PEG_{1000} (□), pure PI (⊞), K80 (circles), and K60 (triangles). TSDC points are also included at $f=1.6$ MHz.

of PEG, the latter as a shoulder on the rising wing of dielectric loss at high temperatures related with Dc conductivity [19]. At lower frequencies the α loss peak is completely masked by conductivity. That is the reason why a rather high frequency (100 Hz), as compared to TSDC (10^{-2}–10^{-4} Hz), was chosen for the isochronal plot in Fig. 5. This difference in frequency is also the reason for the systematic shift of the three loss peaks in Fig. 5 to higher temperatures, as compared to the corresponding TSDC thermogram in Fig. 4.

There are three sources of information from a DRS loss peak recorded at constant temperature, namely the time scale, the magnitude and the shape of the response. These are quantified by fitting the Havriliak–Negami model function [30] to the experimental data.

$$\varepsilon''(\omega) = \mathrm{Im}\left(\varepsilon_\infty + \frac{\Delta\varepsilon}{(1+(i\omega\tau)^\beta)^\gamma}\right) \tag{4}$$

In this equation ω is the angular frequency, $\omega=2\pi f$, $\tau=1/(2\pi f_{HN})$ and f_{HN} a characteristic frequency close to and related with the frequency f_{max} of maximum loss [31], ε_∞ is $\varepsilon'(f)$ for $f\gg f_{HN}$, $\Delta\varepsilon$ the dielectric strength, $\Delta\varepsilon=\varepsilon_s-\varepsilon_\infty$, where ε_s is $\varepsilon'(f)$ for $f\ll f_{HN}$, and β and γ are the shape parameters.

Eq. (4) was fitted to the data for the γ relaxation of PEG and the γ relaxation of PI at several temperatures, typically in step of 10 K, for selected hybrids of the K series. It was found that $\beta=1$, corresponding to a symmetrical relaxation, for both γ relaxations, in agreement with several results for local, secondary relaxations in polymers reported in the literature [19]. $\Delta\varepsilon$ and α were found to change only slightly with temperature.

The most significant information extracted from the HN fits to the experimental data for the two γ relaxations refers to the time scale (f_{HN} and f_{max}) of the response. Fig. 6 shows the Arrhenius diagram (activation diagram), i.e. a plot of $\log f_{max}$ against reciprocal temperature, for the γ relaxation of PEG and the γ relaxation of PI in the two hybrids of the K series with the highest amount of PEG, K80 and K60, as well as for the corresponding pure PI and PEG samples. Included in the plot are also TSDC data, given by the peak temperatures of the corresponding TSDC peaks at the equivalent frequency of $f=1.6$ MHz, corresponding to a relaxation time of 100 s [13,18]. The Arrhenius equation, which is characteristic for local, secondary relaxations in polymers [19],

$$f_{max} = f_0 \exp\left(-\frac{E_{act}}{kT}\right) \tag{5}$$

where f_0 is a constant, E_{act} the apparent activation energy of the relaxation and k Boltzmann's constant, was fitted to the data. The fitting parameters E_{act} and f_0 are listed in Table 2.

We observe in Fig. 6 similar dynamics for the γ relaxation of PEG in the two hybrids and in Table 2 activation parameters which are typical for local, secondary γ relaxations in this temperature region [19]. The TSDC points fit rather well to the extrapolation of the straight Arrhenius lines to lower frequencies/temperatures, bearing in mind the limits in the accuracy of the determination of the TSDC peak temperatures, because of the overlapping with the stronger TSDC peak of the γ relaxation of PI (Fig. 4). Please note that these limits do not apply for the DRS data, as the two γ relaxations do not overlap in the DRS frequency plots because of the different dynamics of the two relaxations to be discussed below. The activation parameters for the γ relaxation of PEG in Table 2 are within the range of values determined for other polyethers and polyesters, e.g. $E_{act}=0.32$ eV (7.38 kcal/mol) and $f_0=4\times10^{12}$ Hz in PIA–PEA hybrid networks; $E_{act}=0.32$ eV (7.38 kcal/mol) and $f_0=5\times10^{13}$ Hz in polyurethanes based on oligotetramethylene glycol [32]. We have included in the Arrhenius diagram also DRS data for the γ relaxation of pure PEG with molar mass 1000 g/mol. They show a slower dynamics of pure PEG, as compared to PEG in the hybrids, in particular at lower frequencies/temperatures. The activation parameters are listed in Table 2. Please note that the values of both apparent activation energy E_{act} and frequency factor f_0 are rather high for one-barrier activation, suggesting some degree of cooperativity [33]. It is interesting to note in this connection that

Table 2
The apparent activation energy E_{act} and the frequency factor f_0 for the secondary relaxations γ PEG and γ PI of selected hybrid networks with short PEG crosslinks (series K) and the pure components PI and PEG of molecular weight 1000 g/mol

Samples	γPI			γPEG		
	E_{act} (eV)	E_{act} (kcal/mol)	f_0 (Hz)	E_{act} (eV)	E_{Acr} (kcal/mol)	f_0 (Hz)
PI	0.51	11.8	8×10^{14}	–	–	–
K60	0.63	14.5	4×10^{16}	0.38	8.76	1×10^{14}
K80	0.65	15.0	3×10^{17}	0.40	9.22	4×10^{14}
PEG_{1000}	–	–	–	0.72	16.6	8×10^{21}

the relaxation strength $\Delta\varepsilon$ does not behave additively in the hybrids, its mean value from measurements at several temperatures being 0.76 in pure PEG, 0.32 in the sample K80 and 0.27 in the sample K60 (without normalization to 100% PEG in the two hybrids). We may speculate, at this stage, that the different dynamics of PEG chains in pure PEG and in the hybrids reflects the different binding properties of the chains, namely fixed covalent bonding to the rigid PIA chains in the hybrids (Scheme 1), as compared to hydrogen bonding of the chain ends in pure PEG.

For the γ relaxation of PI in the two hybrids we observe in Fig. 6 that the TSDC points fit very well to the extrapolation of the DRS Arrhenius lines. The dynamics is rather similar in the two hybrids, by both DRS and TSDC, as indicated also by the values of the activation parameters in Table 2. The dynamics is, however, different in pure PI. In agreement with the TSDC results in Fig. 4, the relaxation is slowed down in the hybrids. The apparent activation energy decreases from 0.63 and 0.65 eV (14.5 and 15.0 kcal/mol) in the two hybrids to 0.51 eV (11.8 kcal/mol) in pure PI. Also, the TSDC point does not correlate well with the DRS data, indicating possibly a change of the dynamics with temperature. It is interesting to note in this connection that in pure PI, in contrast to the hybrids, the γ relaxation could not be fitted by a symmetrical function, the β parameter of the HN expression being significantly smaller than 1, $\beta=0.3$–0.4. The value of 0.51 eV (11.8 kcal/mol) for pure PI is within the range of values determined for the activation energy of the γ relaxation by dielectric and by dynamic mechanical techniques in various PIs [15]. A similar change of dynamics of the γ relaxation of PI in the hybrids, as compared to pure PI, has been observed also in PIA–PEA hybrid networks: the corresponding TSDC peak was found to shift to higher temperatures in the hybrids, whereas the activation energy, determined by DRS, was found to increase from 0.46 eV (10.6 kcal/mol) in pure PI to 0.55 eV (12.7 kcal/mol) in the hybrid with 20 wt% PEA [15].

Contrary to TSDC (Fig. 4), the α relaxation of PEG could not be followed in the DRS frequency spectra, as it was masked by Dc conductivity, appearing only as a weak shoulder in the isochronal plots of some of the hybrids (Fig. 5). This particular difference in resolving power between DRS and TSDC is due to the fact that the steps of polarization and depolarization (in general, stimulus and response, respectively) are separated from each other in TSDC, however not in DRS. In the PIA–PEA hybrids studied before [15], the α relaxation could be easily followed by DRS, as PEA is characterized by much lower conductivity than PEG. An interesting result obtained with those hybrids was that the strength of the α relaxation of PEA decreased with decreasing amount of PEA stronger than additivity would suggest. This result was explained in terms of suppression of the cooperative glass transition due to hybridization [15]. A similar suppression of glass transition was observed by DSC (Fig. 3) in the PIA–PEG hybrids under investigation here. Thus, we may expect that, similar to the PIA–PEA hybrids, the strength of the PEG α relaxation decreases strongly with decreasing amount of PEG in the hybrids, imposing additional difficulties in resolving this relaxation in the DRS spectra.

It is, however, possible, under certain conditions, for a relaxation, where the $\varepsilon''(f)$ loss peak is completely masked by Dc conductivity, to eliminate the conductivity contribution by calculating, by a derivative method, $\varepsilon''(f)$ from the measured $\varepsilon'(f)$, where Dc conductivity makes no contribution [34]. We followed that method and calculated for the hybrid of the K series with the highest amount of PEG (K80) at two temperatures, where the contribution of Dc conductivity to $\varepsilon'(f)$ appeared negligible, $\varepsilon''(f)$ by [34]

$$\varepsilon''_{der} = -\frac{\pi}{2}\frac{\partial\varepsilon'(\omega)}{\partial\ln(\omega)} \approx \varepsilon''_{rel} \tag{6}$$

where $\omega=2\pi f$. The frequency of maximum loss, f_{max}, of the two calculated loss peaks is included in the Arrhenius diagram of Fig. 6, together with the peak temperature of the TSDC α peak of sample K80 from Fig. 4 at the equivalent frequency of 1.6 MHz. Because of the limited number of points (only 3) and the indirect method of calculation, no expression (such as the proper for the glass transition Vogel–Tammann–Fulcher equation) was fitted to the data. We may observe, however, that the data by the two dielectric techniques are roughly in agreement with each other. The TSDC α peak temperature (247 K) agrees rather well also with the DSC glass transition temperature T_g of 252 K (Fig. 3), as already indicated before. It is interesting to note in this connection that in the PIA–PEG hybrids of the K series based on ODPA instead of PMDA, T_g of PEG, determined by dynamic mechanical analysis at 1 Hz, was found to vary in the range 248–265 K [17].

3.3. Crystallization of PEG

Crystallinity of the PEG component in the hybrids was studied by DSC and by DRS. DSC measurements, to be reported in detail elsewhere, showed no crystallization/melting events of PEG in the hybrids with the shorter crosslinks

(K series), in contrast to results obtained with the corresponding pure PEG of molar mass 1000 g/mol. These results are in agreement with similar results obtained with PIA–PEA hybrids at a molar mass of PEA of 1300 g/mol [14] and also with PI-PDMS hybrids [13] and explained in terms of loosened molecular packing of the chains due to hybridization [8].

Crystallization of PEG was observed by DSC in the hybrids with the longer crosslinks (D series) at sufficiently high content of PEG, melting points being in the range 300–330 K. Fig. 7 shows results for the degree of crystallinity of PEG, defined by the ratio of the measured melting enthalpy to the melting enthalpy of a fully crystallized PEG sample [26]. We observe a decreasing degree of crystallinity with decreasing amount of PEG and total suppression of crystallization in the hybrids with the lowest amount of PEG, 20 and 40 wt%. Similarly to other hybrid systems [8], the reduction/suppression of the ability of crystallization of PEG is explained by the presence of the rigid PIA phase limiting long-scale motions of the PEG chains, which are necessary for nucleation and diffusion processes.

There are interesting correlations between the DSC results of PEG crystallization reported above and the DRS data at room temperature reported in Fig. 1. In the samples of the K series ε' was found to increase continuously with increasing PEG fraction (Fig. 1), in good correlation with total suppression of PEG crystallization in these hybrids. In the hybrids with the longer crosslinks (D series), similar results were observed for both ε' and σ_{Ac} (Fig. 1) in the samples D50 and D80. This, unexpected at first glance, result can now be understood, on the basis of Fig. 7, in terms of larger degree of crystallinity of PEG, i.e. reduction of both ε' and σ_{Ac}, in the sample with the higher amount of PEG. Further, the rather large conductivity effects on both $\varepsilon'(f)$ and $\sigma_{Ac}(f)$ for the hybrid D40 in Fig. 1 and, in good correlation with that, the rather high specific heat capacity jump at T_g in Fig. 3 can be naturally explained now as arising from the absence of crystallinity of PEG in this sample (Fig. 7). Finally, one additional observation in Fig. 3, which can now be understood on the basis of the results of Fig. 7, is the slight increase of T_g and the concomitant decrease of the corresponding heat capacity jump for the hybrids of the D series with non-zero degree of crystallinity, i.e. the samples D50, D60 and D80.

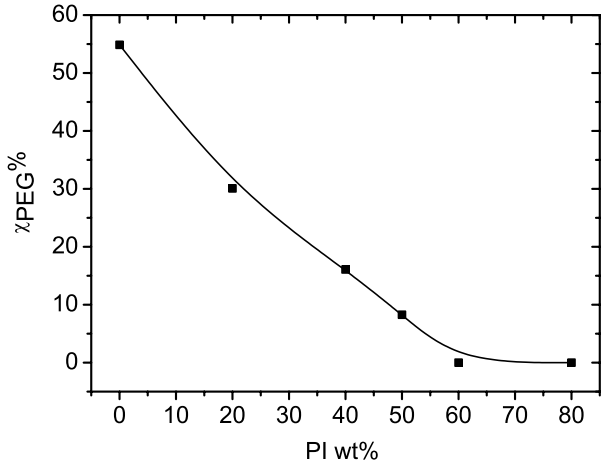

Fig. 7. Degree of crystallinity of the PEG component in the hybrids of the D series, determined by DSC, against PI weight fraction.

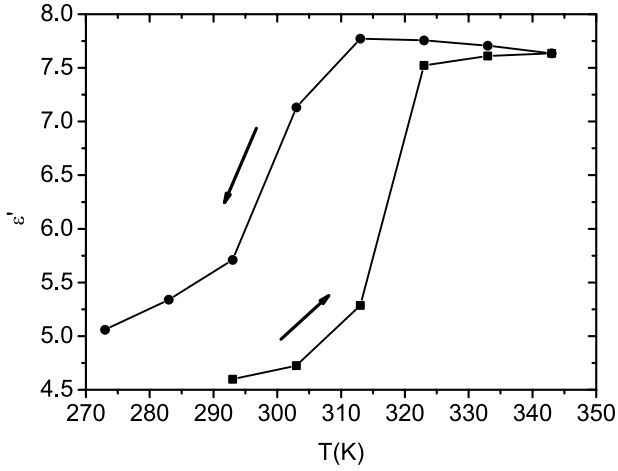

Fig. 8. Isochronal (constant frequency, $f=1$ MHz) plot of ε' versus temperature T for the hybrid network D80 on heating and on subsequent cooling of the sample at a rate of 0.7 K/min.

Crystallization/melting events of PEG in the hybrids have been followed also by DRS. The method is based on the increase of the real part of dielectric permittivity ε' on melting. By making use of the broad frequency range of measurements and the high speed of scanning that range, DRS has been developed to a powerful tool, in particular for studying crystallization kinetics [35]. DSC measurements in the PIA–PEA hybrids [14] had shown a pronounced dependence of melting temperature and melting enthalpy of PEA on heating rate, after cooling rapidly the samples from high temperature to below the crystallization temperature, indicating a strong dependence of the crystallization kinetics on the sample composition.

Fig. 8 shows results of crystallization and melting of PEG in the sample D80: real part of dielectric permittivity ε' against temperature T at selected temperatures in steps of 10 K during heating and cooling of the sample. The temperature history of the sample is here different than in the DSC measurements of Figs. 3 and 7. The sample is heated/cooled at a rate of 0.7 K/min between subsequent temperatures of measurement, where the temperature is kept constant for 10 min for stabilization and measurement of the dielectric properties. At each temperature ε' and ε'' are measured in the frequency range 10^{-1}–10^{7} Hz, before proceeding to the next temperature. A rather high frequency of presentation, 1 MHz, has been selected in Fig. 8, in order to avoid any effects of conductivity on ε'. We observe significant changes of ε' with temperature in the temperature range 313–323 K during heating due to melting of PEG and between 313 and 293 K during cooling due to crystallization of PEG. The large changes in ε'(T) are due to the high polar character of PEG and indicate that DRS is well suited for crystallization studies in the hybrids under investigation. The melting temperature of PEG in the same sample, measured by DSC at a heating rate of 20 K/min, is 320 K, which is within the step 313–323 K obtained by DRS. At the end of the cooling scan ε' has not yet returned to its original value at 293 K prior

to heating, as the sample had been stored for long time at this temperature (room temperature) and crystallization could proceed further.

4. Conclusion

Molecular dynamics, morphology and melting/crystallization phenomena in two series of PIA–PEG hybrid networks with regularly varied composition and different lengths of PEG crosslinks were studied by dielectric techniques (DRS, TSDC), differential scanning calorimetry (DSC) and water uptake measurements.

Long range connectivity of the PEG component was suggested by the characteristics of conductivity and confirmed by water uptake measurements for the hybrid networks with short and long PEG crosslinks at PEG content higher than 40 and 20 wt%, respectively. DSC results showed that the PEG component partially crystallizes in the hybrid networks with the longer PEG crosslinks with more than 40 wt% PEG, only, and that the degree of crystallinity in these samples increases with increasing PEG fraction. The reduction/suppression of crystallization ability of the PEG component in the hybrid networks is explained by the presence of the rigid PIA phase limiting long-scale motions of the PEG chains, which are necessary for nucleation and diffusion processes.

The strength of the secondary γ relaxation of PEG does not behave additively, while that of the secondary γ relaxation of PI increases as PI content decreases. The results reflect the different binding properties of the PEG chains in the hybrid networks, as compared to pure PEG, and the increase of free volume, as a result of the loosening of packing of PI chains in the hybrid networks, respectively.

The T_g of PEG component is shifted to higher temperatures in the hybrids with short PEG crosslinks as compared to the hybrids with longer PEG crosslinks, while the glass transition is totally suppressed in the hybrid networks with short PEG crosslinks and PEG content equal to or lower than 40 wt%. The results can be explained in terms of constraints imposed to segmental motion of the PEG crosslinks by fixing the PEG chain ends on the rigid PI chains.

Acknowledgements

The project is co-funded by the European Social Fund (75%) and National Resources (25%)-(EPEAEK II)-PYTHAGORAS. The work was supported also by the grant Agency of the Czech Republic through the grant No. 104/03/0388.

References

[1] Mittal KL. Polyimides. vol. 1 and 2. New York: Plenum; 1984.
[2] Abadie MJM, Sillion B. Polyimides and other high-temperature polymers. Elsevier: Amsterdam; 1991.
[3] Sindelar V, Sysel P, Hynek V, Friess K, Sipek M, Castaneda N. Collect Czech Chem C 2001;66(33):533–40.
[4] Rogers ME, Rodrigues D, Wilks Gl, MacGrathe JE. Polym Prepr 1991; 32:176.
[5] Schauer J, Sysel P, Marousek V, Pientka Z, Pokorny J, Blecha M. J Appl Polym Sci 1996;61(8):1333–7.
[6] Feng XS, Sourirajan S, Tezel H, Matsuura T. J Appl Polym Sci 1991; 43(6):1071–9.
[7] Deng S, Tremblay A, Matsuura T. J Appl Polym Sci 1998;69(2):371–9.
[8] Bershtein VA, David L, Egorov VM, Pissis P, Sysel P, Yakushev PN. In: Mittal KL, editor. Polyimides and other high temperature polymers, vol. 3. The Netherlands: VSP; 2005. p. 353–99.
[9] Sysel P, Oupicky D. Polym Int 1996;40(4):275–9.
[10] McGrath JE, Dunson DL, Macham SJ, Hedrick JL. Adv Polym Sci 1999; 140:61–105.
[11] Furukawa N, Yamada Y, Furukawa M, Yuasa M, Kimura Y. Polymer 1998;39(13):2941–9.
[12] Brus J, Dybal J, Sysel P, Hobzova R. Macromolecules 2002;35(4):1253–61.
[13] Kripotou S, Pissis P, Bershtein VA, Sysel P, Hobzova R. Polymer 2003; 44(9):2781–91.
[14] Bershtein VA, Egorov VM, Egorova LM, Jakushev PN, David L, Sysel P, et al. Polymer 2002;43(25):6943–53.
[15] Kanapitsas A, Pissis P, Delides CG, Sysel P, Sindelar V, Bershtein VA. Polymer 2002;43(25):6955–63.
[16] Balazs AC. Curr Opin Solid St M 2003;7(1):27–33.
[17] Sysel P, Sindelar V, Hobzova R, Nejedla S, Frycova M. Plasty Kauc 2003; 40:292 [in Czech].
[18] Van Turnhout J. Electrets. In: Sessler GM, editor. Topics in applied physics, vol. 33. Berlin: Springer; 1980. p. 81–215.
[19] Runt JP, Fitzgerald JJ. Dielectric spectroscopy of polymeric materials. Washington, DC: American Chemical Society; 1997.
[20] Pissis P, Kyritsis A, Shilov VV. Solid State Ionics 1999;125(1–4):203–12.
[21] Chen Y, Wang W, Yu W, Yuan Z, Kang ET, Neoh KG, et al. Adv Funct Mater 2004;14(5):471–8.
[22] Funke K, Roling B, Lange M. Solid State Ionics 1998;105(1–5):195–208.
[23] Macedo PB, Moynihan CT, Bose R. Phys Chem Glasses 1972;13(6): 171–9.
[24] Moynihan CT. J Non-Cryst Solids 1994;172:1395–407.
[25] Ferrer GG, Melia JMS, Canales JH, Duenas JMM, Colomer FR, Pradas MM, et al. Colloid Polym Sci 2005;283(6):681–90.
[26] Bershtein VA, Egorov VM, Kemp TJ. Differential scanning calorimetry of polymers. Physics, chemistry, analysis, technology. New York: Ellis Horwood; 1994.
[27] McCrum NG, Read BE, Williams B. Anelastic and dielectric effects in polymeric solids. New York: Wiley; 1967.
[28] Pissis P, Kanapitsas A, Georgoussis G, Bershtein VA, Sysel P. Adv Compos Lett 2002;11(2):49–58.
[29] Vatalis AS, Kanapitsas A, Delides CG, Pissis P. Thermochim Acta 2001; 372(1–2):33–8.
[30] Havriliak Jr S, Havriliak SJ. Dielectric and mechanical relaxation in materials. Munich: Hanser; 1997.
[31] Diaz-Calleja R. Macromolecules 2000;33(24):8924.
[32] Pissis P, Kanapitsas A, Savelyev YV, Akranovich ER, Privalko EG, Privalko VP. Polymer 1998;39(15):3431–5.
[33] Garwe F, Schoenhals A, Beiner M, Schroeter K. Macromolecules 1996; 29(1):247–53.
[34] Wubbenhorst M, van Turnhout J. J Non-Cryst Solids 2002;305(1–3):40–9.
[35] Wurm A, Soliman R, Schick C. Polymer 2003;44:7467–76.